

Are your **MRI contrast agents** cost-effective?

Learn more about generic **Gadolinium-Based Contrast Agents**.



**FRESENIUS
KABI**

caring for life

AJNR

MR appearance of trigeminal and hypoglossal motor denervation.

C P Russo, W R Smoker and J L Weissman

AJNR Am J Neuroradiol 1997, 18 (7) 1375-1383

<http://www.ajnr.org/content/18/7/1375>

This information is current as
of April 18, 2024.

MR Appearance of Trigeminal and Hypoglossal Motor Denervation

Craig P. Russo, Wendy R. K. Smoker, and Jane L. Weissman

PURPOSE: To illustrate and describe the appearance of both long-standing and relatively recently occurring motor denervation of the hypoglossal nerve and of the third (mandibular) division of the trigeminal nerve (V3), with emphasis on findings particular to MR imaging. **METHODS:** Findings from 11 patients with V3 denervation and from seven patients with hypoglossal denervation resulting from a variety of abnormalities were reviewed retrospectively. The motor denervation appearance and functional compromise of the affected musculature are described in terms of the chronicity of the denervation process. **RESULTS:** The appearance of V3 and hypoglossal motor denervation varies with the chronicity of the process. Long-standing denervation results in extensive fatty replacement and a decrease in the size of the affected musculature. Relatively recently occurring denervation results in abnormal contrast enhancement and edemalike signal changes in the denervated musculature. Fatty replacement was observed acutely in hypoglossal denervation but did not manifest until the subacute stage in V3 denervation. Increased volume of the denervated musculature may also accompany acute denervation signal changes. **CONCLUSION:** V3 and hypoglossal denervation have a variable appearance depending on the chronicity of the process. Recognition of MR imaging patterns of denervation may allow earlier diagnosis of a denervating lesion and may help to distinguish denervation from similar-appearing processes, such as infection or neoplasia.

Index terms: Nerves, hypoglossal (XII); Nerves, magnetic resonance; Nerves, trigeminal (V)

AJNR Am J Neuroradiol 18:1375-1383, August 1997

Magnetic resonance (MR) imaging has greatly expanded the capacity to image the cranial nerves directly and to evaluate sequelae of cranial nerve denervation. Harnsberger and Dillon (1) described patterns of cranial nerve motor denervation atrophy seen at computed tomography (CT) and emphasized that these patterns may be the only clue to underlying cranial nerve disease. Recognition of these patterns on CT scans is based on the presence of atrophy and fatty replacement of particular muscle groups. The pathologic process must, therefore, be present for sufficient duration to result in appreciable fatty infiltration and volume loss of the denervated musculature. MR

imaging, with its superior soft-tissue characterization, facilitates recognition of more subtle, earlier fatty infiltration and can show other findings of denervation, such as abnormal muscle enhancement, which are not apparent on CT scans (2, 3).

In our practices we most commonly encounter patients with denervation of the hypoglossal (12th) nerve or of the third (mandibular) division of the trigeminal (fifth) nerve (V3). These nerves are affected by a variety of pathologic processes and the innervated muscle groups are readily recognizable. The purpose of this article is to review the more common MR manifestations of V3 and hypoglossal denervation and to describe the less common manifestations of denervation that are apparent only with MR imaging.

Anatomy

A schematic diagram of the course of the third division of the trigeminal nerve is shown in Figure 1. V3 provides motor innervation to the

Received August 8, 1996; accepted after revision January 24, 1997.

From the Department of Radiology, Medical College of Virginia, Richmond (C.P.R., W.R.K.S.), and the Department of Radiology, University of Pittsburgh (Pa) (J.L.W.).

Address reprint requests to Craig P. Russo, MD, Department of Radiology, Medical College of Virginia, PO Box 980615, Richmond, VA 23298.

AJNR 18:1375-1383, Aug 1997 0195-6108/97/1807-1375

© American Society of Neuroradiology

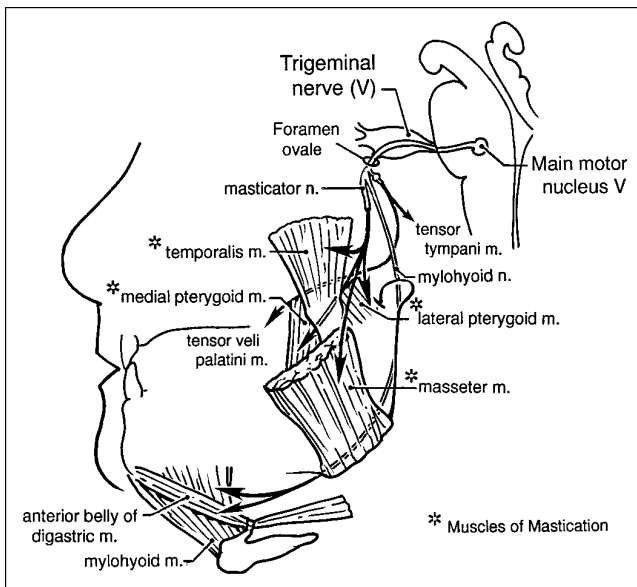


Fig 1. Motor fibers of the mandibular division of the trigeminal nerve (V3). The motor nucleus of the trigeminal nerve is located in the middle pons. The nerve root exits the brain stem at the lateral pons, courses through the prepontine cistern (preganglionic segment), and passes into the gasserian ganglion within Meckel's cave, just lateral to the cavernous sinus. The postganglionic segment trifurcates just distal to the ganglion, and V3 passes inferiorly to exit the skull base via the foramen ovale. V3 enters the masticator space; the motor component divides into two branches: the masticator nerve and the mylohyoid nerve. The masticator nerve supplies the muscles of mastication and the mylohyoid nerve supplies the anterior belly of the digastric and the mylohyoid muscles.

muscles of mastication (temporalis, masseter, medial, and lateral pterygoid) and to two of the muscles of the floor of the mouth (anterior belly of the digastric and mylohyoid). V3 also provides motor innervation to the tensor veli palatini muscle, which regulates eustachian tube patency, and to the tensor tympani muscle, which provides acoustic dampening. Figure 2 is a schematic diagram of the course of the hypoglossal (12th) nerve, which provides motor innervation to the extrinsic muscles of the tongue (genioglossus, hyoglossus, styloglossus, and geniohyoid) and to the intrinsic tongue muscles.

Materials and Methods

We retrospectively reviewed the clinical and teaching files of our institutions and identified 11 cases of V3 denervation and seven cases of hypoglossal denervation. A summary of the cases is presented in Tables 1 and 2, respectively. Imaging patterns were described as acute (less than 1 month), subacute (1 month to 20 months), or chronic (greater than 20 months). Although other authors

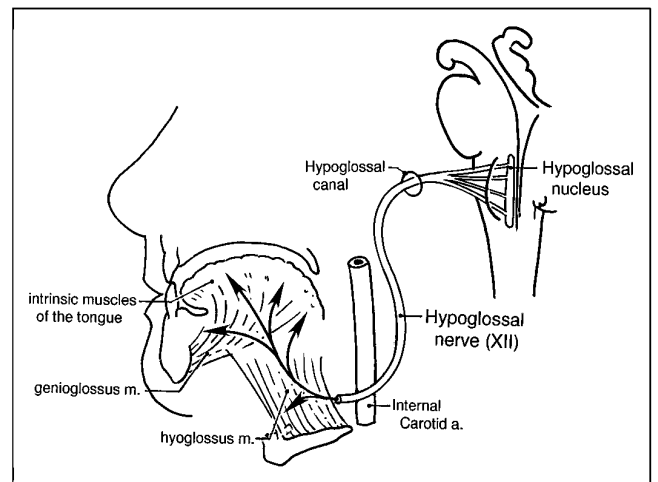


Fig 2. The hypoglossal nuclei are situated just deep to the floor of the fourth ventricle. Multiple 12th nerve rootlets exit the medulla at the preolivary sulcus, in proximity to the vertebral artery, and cross the premedullary cistern to enter the hypoglossal canal. After emerging from the hypoglossal canal, the nerve passes into the carotid space and loops caudally to the level of the hyoid bone. The 12th nerve then courses upward to the sublingual space where it ramifies to supply motor branches to the intrinsic and extrinsic muscles of the tongue.

have arbitrarily defined subacute and chronic differently, our definitions are based on the observation of specific imaging patterns for each of these designations, as described in the "Results" section. Duration of denervation was based on either onset of symptoms or onset of a known pathologic insult (eg, surgical trauma). T2 prolongation of denervated muscles was determined qualitatively by comparing T1- and T2-weighted MR images. T1-weighted images were assessed for fatty infiltration. If the T2-weighted images showed increased signal intensity in addition to, or in a different distribution from, areas of fatty infiltration seen on T1-weighted images, T2 prolongation was considered present. All imaging was done with either a 1.0-T or 1.5-T superconducting magnet, and most examinations included both T1- and T2-weighted images. In several of the cases presented here, contrast material was not administered; and in some cases, only T1- or T2-weighted images were available for review. T2-weighted images were obtained with a conventional spin-echo technique in all but two patients. Fast spin-echo T2-weighted images were obtained in case 7 (Table 1) and fat-suppressed T2-weighted images were obtained in case 6 (Table 2). The greater signal intensity of fat on fast spin-echo images as compared with conventional spin-echo images was not a confounding factor in estimating the presence of T2 prolongation in these patients. In the former patient, T1-weighted images showed no evidence of fatty infiltration; in the latter patient, fat-suppression was used (see Figs 6 and 8). Imaging parameters varied and are provided in the figure legends.

TABLE 1: Patients with V3 denervation

Case	Age, y/ Sex	Symptom/Disease Duration	Pathogenesis	MR Sequences	Fatty Replacement	Enhancement	Increased T2
1	45/F	>3 y	Cavernous sinus meningioma	T1, T2 T1 + contrast	+	-	-
2	39/M	>2 y	Cavernous sinus neuroma (neurofibromatosis type II)	T1, T2 T1 + contrast	+	-	-
3	67/M	...	Fifth nerve neurofibroma	T1, T2	+	...	-
4	56/F	>2 y	Perineural spread of nasopharyngeal adenoid cystic carcinoma	T1, T2 T1 + contrast	+	-	-
5	75/F	...	Cavernous sinus meningioma	T1, T2 T1 + contrast	+	-	-
6	54/F	>16 mo	Recurrent cerebellopontine angle meningioma	T1, T2 T1 + contrast	+	+	-
7	27/M	2 d	Cavernous sinus lymphoma	T1, T2 T1 + contrast	-	+	+
8	49/F	2 wk	Lung metastasis to cavernous sinus	T1, T2 T1 + contrast	-	+	+
9	37/F	20 mo	Brain stem cavernous hemangioma	T1, T2 T1 + contrast	+	+	+
10	47/M	6 mo	Perineural spread of adenoid cystic carcinoma	T1, T2 T1 + contrast	+	+	+
11	.../F	8 mo	Cavernous sinus meningioma	T1, T2 T1 + contrast	+	+	+

* Enhancement was no longer present at 20 months.

TABLE 2: Patients with hypoglossal denervation

Case	Age, y/Sex	Symptom/Disease Duration	Pathogenesis	MR Sequences	Fatty Replacement	Enhancement	Increased T2
1	55/M	...	Skull base meningioma	T1, T2	+	...	-
2	16/M	Several years	12th nerve schwannoma (neurofibromatosis type II)	T1, T2 T1 + contrast	+	-	-
3	74/M	1 mo	Nasopharyngeal squamous cell carcinoma with skull base invasion	T1, T2	+	...	+
4	29/F	2 wk	Recent tonsillectomy	T1	+
5	78/M	1.5 mo	Colon metastasis to skull base	T1	+
6	70/M	Several weeks	Recurrent laryngeal carcinoma at carotid sheath with recent radiation therapy	T1, T1 + contrast T2	+	+	+
7	24/F	3 wk	Surgical trauma	T1 + contrast, T2	?*	?*	+

* Increased signal intensity was present on T1 + contrast images, which may have represented fatty change, enhancement, or both.

Results

V3 Denervation

Images of patients with V3 denervation exhibited one of four patterns: 1) long-standing chronic denervation, characterized by extensive fatty infiltration and volume loss of denervated musculature, without evidence of abnormal muscle enhancement or T2 prolongation; 2) early/mild chronic denervation, characterized by mild fatty change of the affected muscula-

ture without appreciable volume loss, evidence of T2 prolongation, or abnormal enhancement; 3) subacute denervation, characterized by abnormal enhancement, T2 prolongation, and fatty replacement of the denervated muscles, without increase in muscle volume; or 4) acute denervation, characterized by abnormal muscle enhancement, T2 prolongation, increase in muscle volume, but no fatty infiltration.

Four of 11 patients (Table 1, cases 1-4) had findings consistent with long-standing chronic

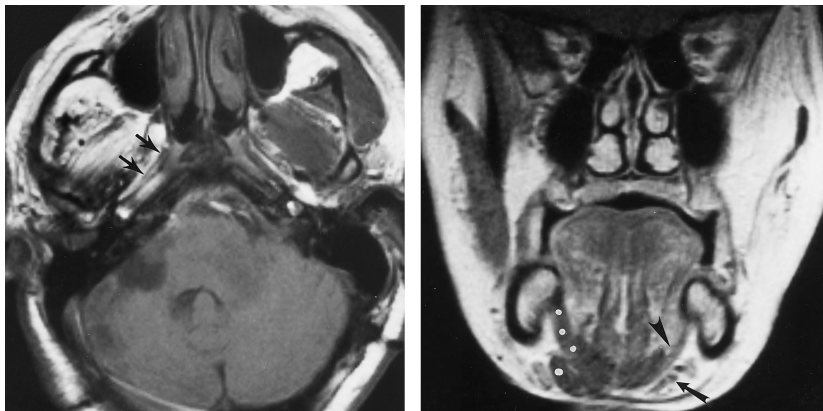


Fig 3. Long-standing chronic V3 denervation.
A, Axial T1-weighted image (600/15/2 [repetition time/echo time/excitations]) shows extensive fatty infiltration and volume loss of the right-sided muscles of mastication. Note the thinned atrophic appearance of the tensor veli palatini muscle (*arrows*).
B, Coronal T1-weighted image (600/17/1) in a different patient shows the atrophic left anterior belly of the digastric (*arrow*) and mylohyoid (*arrowhead*) muscles. The normal right-sided digastric (*large dot*) and mylohyoid (*small dots*) muscles are indicated.-

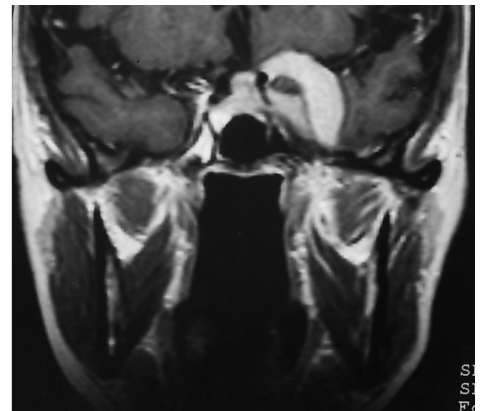


Fig 4. Early, less severe chronic V3 denervation atrophy. Coronal contrast-enhanced T1-weighted image (630/17/1) shows a left cavernous sinus region meningioma. Note linear areas of increased signal intensity in the ipsilateral pterygoid muscles, consistent with fatty change, and relative preservation of muscle volume. The unenhanced T1-weighted image (not shown) had the same appearance.

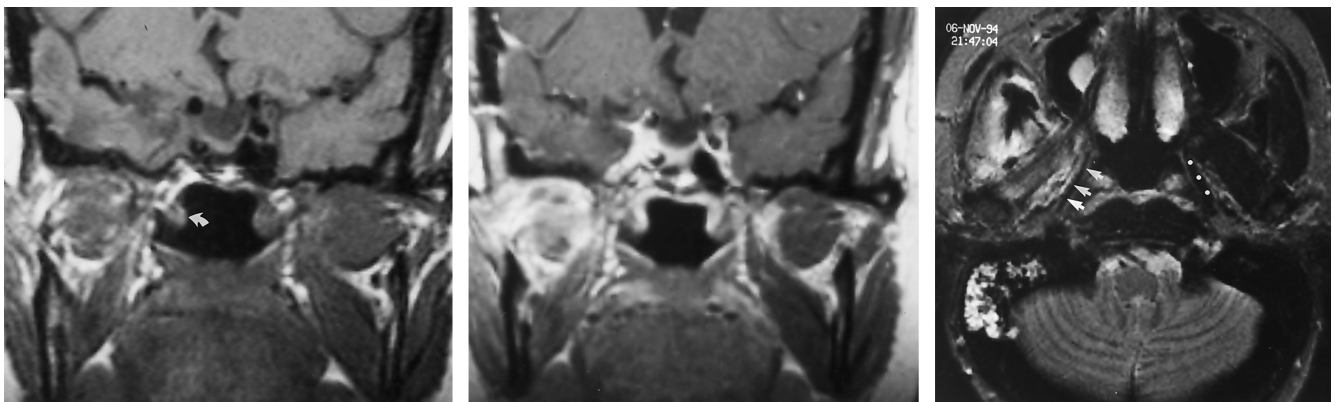


Fig 5. Subacute V3 denervation.
A, Coronal T1-weighted image (600/20/3) shows fatty infiltration and some volume loss of the right-sided muscles of mastication. Note a small ipsilateral torus tubarius, which may be related to tensor veli palatini dysfunction (*arrow*).
B, Coronal contrast-enhanced T1-weighted image (700/22/1) at approximately the same level as **A** shows enhancement of the muscles of mastication.
C, Axial T2-weighted image (2500/90/1) shows mastoid air cell fluid, consistent with tensor veli palatini dysfunction. Also note edemalike increased signal intensity in the right-sided muscles of mastication, especially the temporalis and masseter. Also note the small size of the right-sided tensor veli palatini muscle (*arrows*) as compared with the normal left side (*dots*).

denervation atrophy (Fig 3). Three of these patients had symptoms of a known disease process of greater than 2 years' duration. Clinical history was not available in one patient. Three of the four patients with the long-standing chronic denervation pattern were examined with T1-weighted imaging with and without contrast enhancement and with T2-weighted imaging. Contrast-enhanced images were not available in case 3.

Only one patient (case 5) had findings consistent with earlier or less severe chronic denervation (Fig 4). Although the available clinical history was inadequate to determine the chronicity of the process in this patient, the size of the meningioma responsible for the denervation indicated a duration of months to years (Fig 4). In four of 11 patients (cases 6 and 9-11), symptom duration ranged from 6 to 20 months, and the images showed a subacute denervation

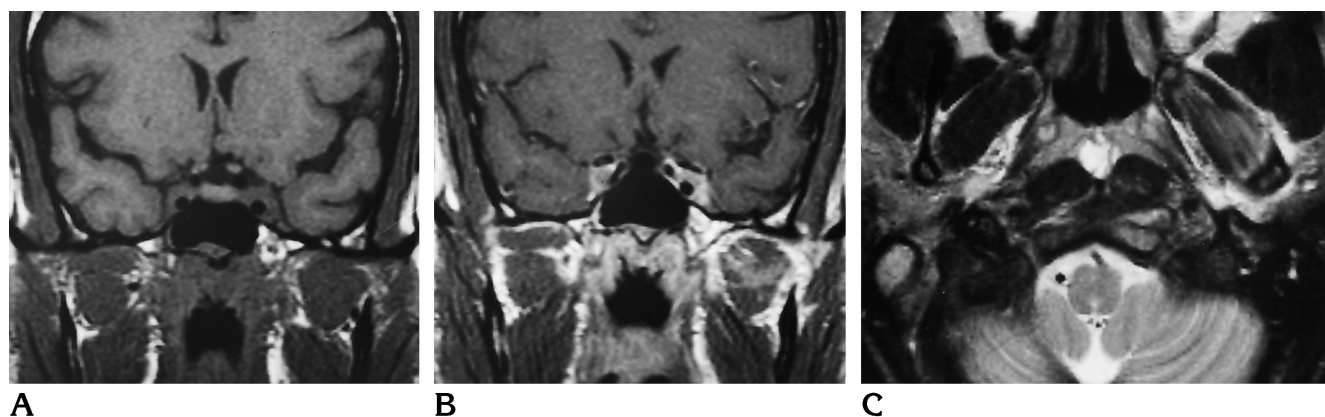


Fig 6. Acute V3 denervation.

A, Coronal unenhanced T1-weighted image (500/15/3) shows no evidence of fatty infiltration of the left-sided muscles of mastication.

B, After contrast enhancement, T1-weighted image (528/17/3) at the same level shows patchy contrast enhancement of the left-sided lateral pterygoid muscle.

C, Axial turbo T2-weighted image (4000/90/1, echo train = 5) shows edemalike increased signal intensity in the left lateral pterygoid muscle and slight increased muscle volume.

pattern (Fig 5). In case 11, postoperative follow-up imaging at 20 months revealed persistent masticator muscle atrophy with resolution of the abnormal enhancement observed at 8 months, consistent with transition to a chronic denervation appearance.

The remaining two of 11 patients (cases 7 and 8) presented acutely, after 2 days and 2 weeks of symptoms, respectively, and had findings of acute denervation (Fig 6).

Indirect findings of V3 denervation were also observed. One patient had a small torus tubarius on the affected side and ipsilateral mastoiditis, both consistent with loss of tone at the opening of the eustachian tube, related to tensor veli palatini dysfunction (Fig 5).

Hypoglossal Denervation

Images of patients with hypoglossal denervation showed patterns similar to those observed for trigeminal denervation, although fatty infiltration appeared to occur earlier in hypoglossal denervation. No distinct early/mild chronic hypoglossal denervation pattern was identified. Two of the seven patients with hypoglossal denervation had findings consistent with long-standing chronic denervation. One of these patients (case 2, Table 2) had symptoms of several years' duration, related to a long-standing hypoglossal schwannoma. The second patient had a long-standing densely calcified skull base meningioma; clinical history was insufficient to specify a more exact duration of symptoms. Images in both these patients showed

extensive fatty replacement of the affected hemitongue, with loss of normal tongue muscle volume (Fig 7). Prolapse of the affected hemitongue into the oropharynx was consistent with loss of normal tongue muscle tone. There was no edemalike T2 prolongation of the tongue in either case, and the one contrast-enhanced study showed no abnormal enhancement.

Five of seven patients (cases 3–7), with symptom duration ranging from 2 to several weeks, had findings consistent with acute/subacute denervation. Acute and subacute hypoglossal denervation are considered together, as these stages exhibited the same imaging pattern. One patient (case 6) was examined with T1-weighted imaging, with and without contrast enhancement, and with fat-suppressed T2-weighted imaging. This patient's images showed fatty infiltration of the denervated hemitongue as well as abnormal enhancement and edemalike T2 prolongation (Fig 8). Three other patients with subacute symptom duration were examined with T1-weighted imaging without contrast administration. Images in all three patients showed varying degrees of fatty replacement of the denervated hemitongue. T2-weighted images were available in three (cases 3, 6, and 7) of the five patients with acute/subacute denervation, and edemalike T2 prolongation was observed in all three cases. Hemitongue swelling was observed in cases 4 and 7 (Fig 9). Increased signal intensity was seen on contrast-enhanced T1-weighted images in case 7. It could not be determined whether this represented enhancement or fatty infiltration, given

Fig 7. Long-standing chronic hypoglossal denervation atrophy. Axial (A) and coronal (B) T1-weighted images (680/20/1) show extensive increased signal intensity of the left hemitongue, reflecting extensive fatty replacement. Note prolapse of the hemitongue into the oropharynx, indicating loss of normal muscle tone.

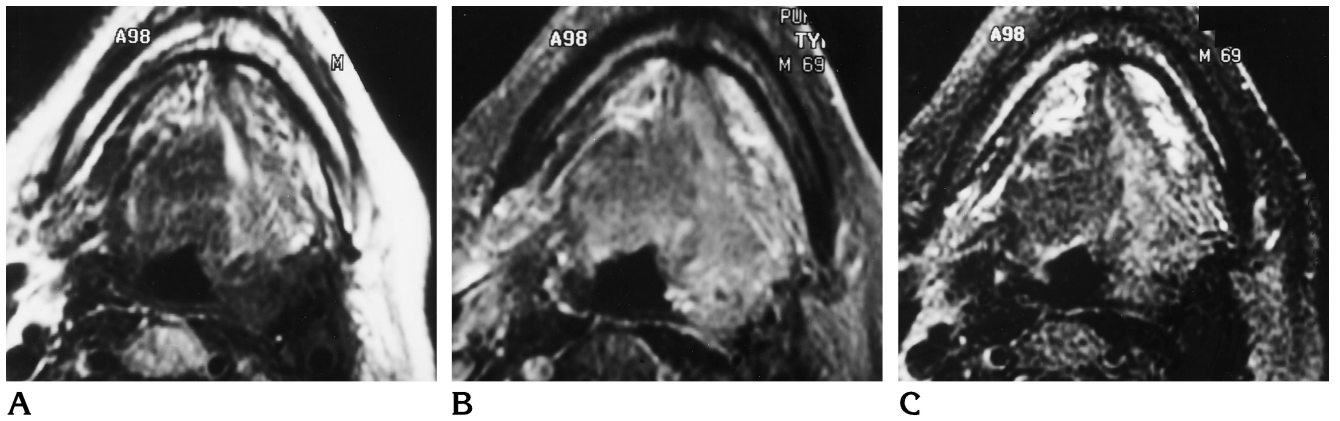
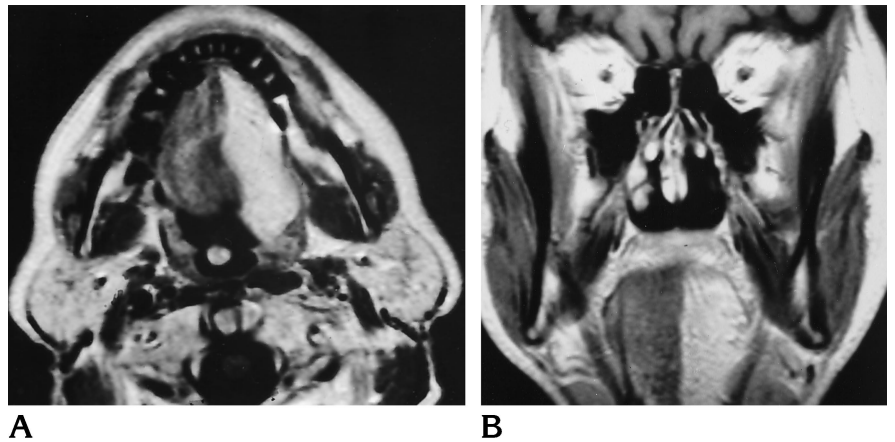


Fig 8. Acute/subacute hypoglossal denervation.

A, Unenhanced axial T1-weighted image (566/19/2) shows increased signal intensity of the left hemitongue, reflecting fatty infiltration.

B, Contrast-enhanced axial fat-suppressed T1-weighted image (549/38/2) at the same level as A shows enhancement of the left hemitongue.

C, Fat-suppressed fast spin-echo T2-weighted image (3000/91/1, echo train = 8) shows edemalike increased signal intensity of the denervated left hemitongue.

that no unenhanced T1-weighted images were obtained.

Discussion

MR signal abnormalities in denervated skeletal muscle have been described for both peripheral (4–7) and cranial (2, 3, 8) nerves. Some findings, such as extensive fatty infiltration, seen in long-standing denervation atrophy may be readily apparent on CT scans (1). MR images, however, can show findings that occur earlier in the denervation process, before severe muscle atrophy is apparent. On the basis of our own observations, along with findings from previous experimental and clinical studies, we have

categorized the appearance of denervation roughly according to the chronicity of the process. Both V3 and hypoglossal denervation can be described in terms of chronic, subacute, or acute denervation, each with a distinctive set of imaging features.

Long-standing chronic V3 and hypoglossal denervation were manifested by marked loss of volume of the affected musculature with extensive fatty replacement (Figs 3 and 7). These findings are identical to those observed on CT scans (1). Secondary findings of ipsilateral mastoiditis and asymmetry of the torus tubarius were also observed in V3 denervation (Fig 5). Mastoiditis is consistent with loss of regulation of the eustachian tube related to tensor veli

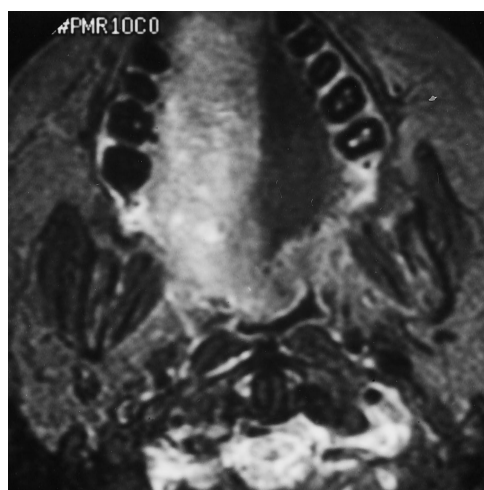


Fig 9. Acute hypoglossal denervation. Axial fast spin-echo T2-weighted image (2600/95/1, echo train = 8) shows swelling and edema-like increased signal intensity of the right hemitongue. Note protrusion of the hemitongue across the midline and posteriorly into the oropharynx.

palatini denervation. The pathogenesis of torus tubarius asymmetry is unclear given that most of the torus is made up of fibers from the levator veli palatini, which is innervated by the vagus nerve. There was no evidence of vagus nerve denervation in the case illustrated. Perhaps loss of tone in tensor veli palatini muscle fibers inserting at the eustachian tube altered the appearance of the torus tubarius. Prolapse of the hemitongue into the oropharynx on axial supine imaging was observed in hypoglossal denervation and was consistent with loss of normal tongue muscle tone. In those cases of V3 and hypoglossal denervation in which there was extensive fatty replacement of the affected musculature, neither abnormal muscle enhancement nor increased signal intensity on T2-weighted images was observed. The exact duration of denervation necessary to produce this pattern of atrophy is unclear. One patient, with findings of subacute denervation at 8 months, had a chronic denervation pattern on a repeat MR examination at 20 months. Long-term serial scanning was not performed in our remaining cases and we were, therefore, unable to follow patients through the stages of denervation beginning at the onset of disease or of symptoms. Also, the clinical history that was available in patients with a pattern of long-standing chronic denervation atrophy was insufficient to allow accurate determination of the onset of clinical symptoms. Studies of experimentally created denervation in animal models

have focused on early biochemical and MR changes in denervated muscle, but serial studies of the appearance of denervated muscle over a period of months to years have not been performed (9–12). Clinical studies that define the beginning of denervation as the onset of symptoms are also inherently limited given that the temporal relation of the denervation process to the onset of symptoms is variable (6). In our series, all patients with a pattern of long-standing chronic denervation and determinable clinical history had symptoms or a known pathologic process of at least 20 months' duration. The minimum duration necessary for this appearance could not be determined.

We also observed a more subtle, but similar, appearance of V3 denervation atrophy, consistent with early or mild chronic denervation (Fig 4). In both long-standing and early chronic denervation, images showed evidence of fatty replacement of the denervated musculature, but fatty replacement in the latter was much less extensive. Muscle volume was relatively preserved in early chronic denervation and there was no evidence of abnormal muscle enhancement or edema-like increased signal intensity on T2-weighted images.

In patients with symptoms ranging from 2 days to 20 months duration, we observed imaging patterns consistent with acute/subacute denervation, as has been described by other authors (2, 4, 7). One feature of these patterns was T2 prolongation of the denervated musculature. Polak et al (5) observed similar T2 prolongation in an animal model 2 weeks after sciatic nerve ligation. Analysis of the denervated muscle revealed no change in overall water content, but there was a relative increase in extracellular water with a concomitant decrease in intracellular water, which coincided with a decrease in muscle fibril size. An increase in extracellular water, which has a longer T2 than intracellular water, most likely accounts for increased T2 signal intensity in the acute/subacute stage. As emphasized by Fleckenstein et al (4), it may be useful to consider the T2 prolongation observed in acute/subacute denervation to be edema-like rather than as reflecting true edema, given that true edema implies an absolute increase in tissue water content. On the other hand, the increased muscle volume seen in several of our cases of acute/subacute trigeminal and hypoglossal denervation suggests there may be a component of true edema

as well. STIR (short-tau inversion-recovery) imaging appears to be especially sensitive to T1 and T2 prolongation associated with acute/subacute denervation (4, 7). For example, West et al (7) found increased STIR signal as early as 4 days after onset of clinical symptoms of denervation, which preceded changes on electromyography. Other authors have observed a similar pattern of masticator subacute denervation several months after the onset of denervating disease (2, 8).

The presence of increased contrast enhancement in acute/subacute denervation may also be attributable to an increase in extracellular space. Contrast material normally distributes between the intravascular and extracellular spaces. The expanded extracellular space in acutely/subacutely denervated muscle therefore allows for more contrast accumulation (2). Animal studies have also found that denervated muscle has relatively increased vascularity per volume of muscle, although this luxury perfusion is somewhat diminished by capillary necrosis (9–12). This relatively increased perfusion may also contribute to increased contrast enhancement.

In our series, the images of the two patients with acute symptoms of V3 denervation showed abnormal enhancement, increased volume, and T2 prolongation of the muscles of mastication, but no fatty replacement. Images in the patients with subacute V3 denervation showed fatty replacement as well as abnormal enhancement and T2 prolongation of the denervated musculature without increase in muscle volume. Images of the patients with subacute V3 denervation, therefore, had an appearance of combined features of the acute and chronic stages. This suggests that there is a continuum in the patterns of denervation such that fatty replacement gradually develops and abnormal enhancement decreases with increasing duration of the process. Indeed, in one patient with a typical pattern of subacute denervation at 8 months, images showed a typical appearance of chronic denervation at 20 months.

Imaging findings in acute/subacute hypoglossal denervation were similar to those observed in V3 denervation, although fatty replacement appeared earlier (Fig 8). Abnormal enhancement and an edemalike appearance were also observed, although the limited imaging in our small number of patients prevents any

conclusions about the frequency of these findings.

Familiarity with findings in acute/subacute denervation is important in that inflammatory or neoplastic processes may have a similar appearance. Awareness of the presence of abnormal enhancement and an edemalike appearance in acute/subacute denervation should direct one to look for a denervating lesion. Denervation may appear almost identical to inflammatory or neoplastic processes when muscle swelling is present. Denervation pseudohypertrophy, characterized by an increase in muscle volume attributable to fatty infiltration, may also appear similar to acute/subacute denervation as described here, especially in the tongue (13). In our series, T2-weighted images in patients with increased muscle volume showed edemalike features, which are not characteristic of denervation pseudohypertrophy. True denervation hypertrophy, characterized by muscle enlargement without signal abnormality, has been reported in the radiologic literature (13). In contradistinction to findings in true denervation hypertrophy, the images in our patients with muscle enlargement all showed signal abnormality.

In summary, imaging findings in V3 and hypoglossal denervation depend on the chronicity of the process. In the acute to subacute stage, the denervated muscles may show increased signal intensity on T2-weighted images, increased muscle volume, and abnormal contrast enhancement. Fatty infiltration was not observed in V3 denervation in the acute stage but was present in subacute V3 denervation and in both acute and subacute hypoglossal denervation. Chronic denervation may be divided into early/mild and long-standing, depending on the amount of fatty infiltration present. In early chronic denervation, mild fatty replacement may be seen without appreciable muscle volume loss, abnormal enhancement, or T2 prolongation. Long-standing chronic cases demonstrated extensive fatty replacement and volume loss of the denervated musculature. Further research may more definitively define the time course of these changes.

References

1. Harnsberger HR, Dillon WP. Major motor atrophic patterns in the face and neck: CT evaluation. *Radiology* 1985;155:665–670
2. Davis SB, Mathews VP, Williams DW. Masticator muscle enhancement in subacute denervation atrophy. *AJNR Am J Neuroradiol* 1995;16:1292–1294

3. Hutchins LG, Harnsberger HR, Hardin CW, et al. The radiologic assessment of trigeminal neuropathy. *AJNR Am J Neuroradiol* 1989;10:1275-1282
4. Fleckenstein JL, Watumull D, Conner KE, et al. Denervated skeletal muscle: MR imaging evaluation. *Radiology* 1993;187:213-218
5. Polak JF, Jolesz FA, Adams DF. Magnetic resonance imaging of skeletal muscle prolongation of T1 and T2 subsequent to denervation. *Invest Radiol* 1988;23:365-369
6. Uetani M, Hayashi K, Matsunaga N, et al. Denervated skeletal muscle: MR imaging. *Radiology* 1993;189:511-515
7. West GA, Haynor DR, Goodkin R, et al. Magnetic resonance imaging signal changes in denervated muscles after peripheral nerve injury. *Neurosurgery* 1994;35:1077-1085
8. Shellhas KP. MR imaging of muscles of mastication. *AJR Am J Roentgenol* 1989;153:847-855
9. Bondy SC, Purdy JL, Carroll JE, et al. The rate of nutrient supply to normal and denervated slow and fast muscle, and its relation to muscle blood flow. *Exp Neurol* 1976;55:678-683
10. Carpenter S, Karpati G. Necrosis of capillaries in denervation atrophy of human skeletal muscle. *Muscle Nerve* 1982;5:250-254
11. Hassler O. The angioarchitecture of normal and denervated skeletal muscle. *Neurology* 1970;20:1161-1164
12. Hudlicka O. Blood flow and oxygen consumption in muscles after section of ventral roots. *Circ Res* 1967;20:570-577
13. Petersilge CA, Pathria MN, Gentili A, et al. Denervation hypertrophy of muscle: MR features. *J Comput Assist Tomogr* 1995;19:595-600